



Elucidating ligand effects in rhodium(III)-catalyzed arene–alkene coupling reactions

Kongchuan Wu^{a,1}, Dandan Lu^{a,1}, Jianbin Lin^a, Ting-Bin Wen^a, Wei Hao^{b,*}, Kai Tan^{a,*}, Hui-Jun Zhang^{a,*}

^a Department of Chemistry, College of Chemistry and Chemical Engineering, Xiamen University, Xiamen 361005, China

^b Beijing National Laboratory for Molecular Sciences, CAS Key Laboratory of Molecular Recognition and Function, Institute of Chemistry, Chinese Academy of Sciences (CAS), Beijing 100190, China

ARTICLE INFO

Article history:

Received 28 May 2023

Revised 3 August 2023

Accepted 5 August 2023

Available online 9 August 2023

Keywords:

Organometallics

Transition metal catalysis

Arene–alkene coupling

β -H elimination

Rhodium hydride

ABSTRACT

Rhodium(III)-catalyzed C–H couplings of arenes with alkenes are among the most powerful methods for C–C bond formation. For these transformations, subtle manipulation of ancillary ligands can lead to dramatic changes in reactivity and selectivity. However, detailed mechanistic studies concerning the ligand effects are rare. In this study, we investigated the origin of ligand-controlled product-selectivity in rhodium(III)-catalyzed C–H couplings of arenes with alkenes, using a series of well-defined $[\text{Cp}^X\text{Rh}^{\text{III}}]$ complexes that feature electronically or sterically distinct Cp^X (Cp ($\eta^5\text{-C}_5\text{H}_5$), Cp^{CF_3} ($\eta^5\text{-C}_5\text{Me}_4\text{CF}_3$) and Cp^* ($\eta^5\text{-C}_5\text{Me}_5$)) ligands. A combination of experimental and theoretical investigations showed that (i) rhodium hydride species containing the electron rich Cp^* ligand can undergo reinsertion of the alkene, thereby allowing rhodium-walking, (ii) rhodium hydride species involving the electron-deficient Cp or Cp^{CF_3} ligands prefer reductive elimination rather than alkene insertion. These findings offer valuable insights on future rational catalyst design for selective arene–alkene cross coupling reactions.

© 2024 Published by Elsevier B.V. on behalf of Chinese Chemical Society and Institute of Materia Medica, Chinese Academy of Medical Sciences.

As powerful methods for C–C bond formation, C–H couplings of arenes with alkenes have been actively studied using a broad range of transition-metal catalysts (e.g., Pd, Rh, Ru and Ir) [1–5]. Nevertheless, many important mechanistic details with respect to ligand effects remain largely unknown [6–12]. Metal hydride species are often proposed as crucial intermediates relevant to product-determining steps in these transformations [13–22], yet in-depth investigations on their formation and reactivities are scarce [23,24]. In recent years, a variety of well-defined rhodium(III) complexes with electronically and sterically tuned cyclopentadienyl (Cp^X) ligands have proven to be efficient catalysts for arene–alkene coupling reactions [25–33]. Subtle manipulation of the Cp^X ligands can result in significant changes in reactivity and selectivity. For instance, as depicted in Scheme 1, the reaction of arenes with vinyl esters under $[\text{Cp}^*\text{Rh}^{\text{III}}]$ catalysis leads to the selective formation of vinyl arenes [29], while $[\text{CpRh}^{\text{III}}]$ can catalyze dehydrogenative alkenylation of arenes [30]. The reason for such a dichotomy in product distribution remains unclear. We also question whether

this kind of ligand-tuned selectivity is widespread in other arene–alkene coupling reactions.

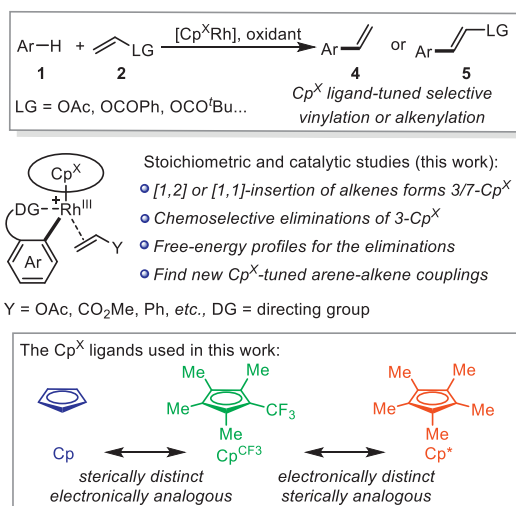
Herein, we present a comprehensive mechanistic study of the C–H coupling reactions of benzamides with alkenes, such as vinyl acetate and methyl acrylate. These reactions were catalyzed by three distinct $[\text{Cp}^X\text{Rh}^{\text{III}}]$ catalysts (Scheme 1), where Cp^X represents Cp , Cp^{CF_3} and Cp^* [34–36]. Our study demonstrated that the Cp ligand, which is more electron-deficient and less sterically hindered than Cp^* ligand, can readily facilitate β -H elimination and the following reductive elimination of the corresponding rhodium hydride species. In contrast, rhodium hydride species containing the electron rich Cp^* ligand tend to undergo reinsertion of the alkene, thereby enabling rhodium-walking. Based on these mechanistic findings, we have also developed several novel ligand-directed divergent arene–alkene coupling reactions.

We first synthesized and isolated three seven-membered rhodacycles **3-Cp***, **3-Cp^{CF3}** and **3-Cp**, as shown in Fig. 1. These complexes are believed to be crucial intermediates in the $[\text{Cp}^X\text{Rh}^{\text{III}}]$ -catalyzed C–H couplings of benzamides with vinyl acetate [5,27–33]. Stoichiometric reactions of $[\text{Cp}^*\text{RhCl}_2]_2$, $[\text{Cp}^{\text{CF}_3}\text{RhCl}_2]_2$ and $[\text{CpRh}_2]_n$ with benzamide **1a** and vinyl acetate **2a** were performed in acetone. We added 1.0 equiv. of NaOAc and 2.1 equiv. of AgSbF_6 to the reaction systems to promote C–H rhodation [37,38] and en-

* Corresponding authors.

E-mail addresses: weihao@iccas.ac.cn (W. Hao), ktan@xmu.edu.cn (K. Tan), meghjzhang@xmu.edu.cn (H.-J. Zhang).

¹ These authors contributed equally to this work.



Scheme 1. Study on ligand effects in Rh(III)-catalyzed arene-alkene coupling reactions.

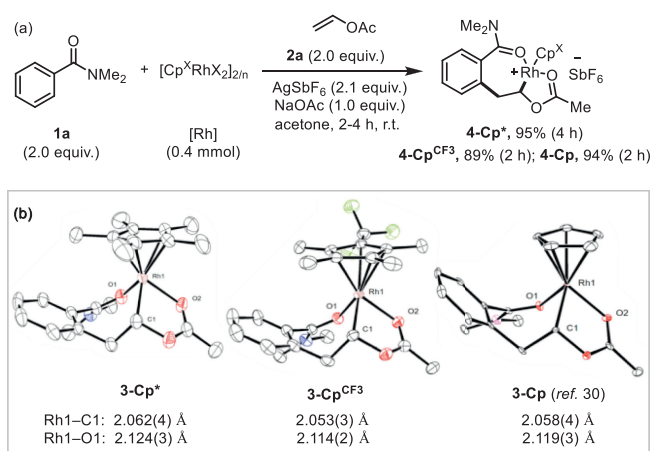


Fig. 1. (a) Syntheses of seven-membered rhodacycles **3-Cp^{*}**, **3-Cp^{CF3}** and **3-Cp**. (b) X-ray crystal structures of **3-Cp^{*}**, **3-Cp^{CF3}** and **3-Cp**. Thermal ellipsoids are drawn at 50% probability. H atoms and SbF₆⁻ anions have been omitted for clarity.

hance the reactivity of corresponding cyclometalated Rh intermediates [39,40]. After stirring the reaction systems at room temperature for 2–4 h, we were able to isolate **3-Cp^{*}**, **3-Cp^{CF3}** and **3-Cp** in high yields of 95%, 89% and 94%, respectively. Their ¹H NMR spectra display ddd multiplets (δ 6.30 (**3-Cp^{*}**), 6.75 (**3-Cp^{CF3}**) and 8.08 (**3-Cp**) for methine groups that are connected to the rhodium centers. The corresponding ¹³C NMR signals appear at δ 105.5, 105.0 and 97.5 (doublet, $^1J_{\text{Rh-C}} = 31.1, 28.1, 25.6$ Hz). The ¹H NMR signals of Cp^{*} ligands in **3-Cp^{*}** and Cp ligand in **3-Cp** appear at δ 1.29 (singlet) and 5.01 (doublet, $^2J_{\text{Rh-H}} = 0.8$ Hz), respectively. The Cp^{CF3} ligand in **3-Cp^{CF3}** displays an unusual set of four singlets, indicating four inequivalent methyl groups with different environments. The structures of **3-Cp^{*}**, **3-Cp^{CF3}** and **3-Cp** were all unambiguously confirmed by single-crystal X-ray diffraction analyses (Fig. 1b). The Rh-C and Rh-O distances decrease with an increase in the electron-deficiency of Cp^X ligands. These complexes are stable upon exposure to air for a few months perhaps due to extra coordination interactions between the rhodium centers and ester carbonyl groups. The molecular structures of **3-Cp^{*}**, **3-Cp^{CF3}** and **3-Cp** suggest a selective [1,2]-insertion of vinyl acetate into the Rh-C bonds of cyclometalated intermediates during the catalytic cycle.

The elimination reactions of the three alkene insertion intermediates **3-Cp^X** were then investigated to determine the origin of se-

lective vinylation or alkenylation (Fig. 2). Since the catalytic C–H couplings of arenes with alkenes are typically performed in the presence of Cu(OAc)₂, acetate salts such as NBu₄OAc and NaOAc were added (Fig. 2a, Figs. S8 and S13 in Supporting information) [5,27–33]. In the presence of highly soluble NBu₄OAc, **3-Cp^{*}** quickly underwent elimination at room temperature to produce vinyl arene **4a** and Cp^{*}Rh^{III}(OAc)₂ (**6-Cp^{*}**) in high yields (Fig. 2a). In contrast, treatment of **3-Cp** with NBu₄OAc mainly afforded alkenyl arene **5aa** and a unique dimeric Rh(II) complex **6'-Cp**. Simultaneous formation of hydrogen gas was also observed by gas chromatography (Fig. S12 in Supporting information). The structure of **6'-Cp** was confirmed by single-crystal X-ray diffraction analyses (Fig. 2a). We have also determined that **6'-Cp** is a catalytically competent species in the arene-alkene couplings (Table S1 in Supporting information). These results indicate facile reductive elimination of corresponding [CpRh-H] intermediates in the catalytic cycle [41,42], although an acetate-promoted E2-type elimination cannot totally be excluded [43]. Similarly, addition of acetate salt also enabled the elimination of **3-Cp^{CF3}** at room temperature, producing vinyl arene **4a** and alkenyl arene **5aa** in a ratio of 1:2. When the reaction was performed at 80 °C, this ratio as well as the conversion of **3-Cp^{CF3}** increased dramatically (Fig. S8 in Supporting information). We monitored these elimination processes by *in situ* ¹H NMR spectroscopy. The kinetic profiles of the elimination reactions are displayed in Figs. 2b–d. The significant electronic effects of Cp^X ligands on product selectivities of the catalytic reactions were evident from the distinct initial rates of product formation (Fig. S9 in Supporting information).

Computational studies were also conducted on the elimination process using the Gaussian 16 program package [44]. Fig. 3 illustrates the energy profiles for **3-Cp**, and additional energy values for the elimination processes of **3-Cp^{*}** and **3-Cp^{CF3}** are also included. By exploring the potential energy surface, it is possible to locate stationary points and transition states that could give rise to rhodium-hydride intermediates **IntB-Cp^X**, which in turn can lead to the formation of both **5aa** (path i) and **4a** (path ii). The transition state **TS1** for *cis*- β -hydride elimination of **3-Cp^X** is markedly stabilized by the unsubstituted Cp ligand. In path i, the rhodium-hydride intermediate **IntB-Cp** can undergo reductive elimination via **TS2** (with a free energy barrier of 4.72 kcal/mol) to generate **5aa** and **6'-Cp**. Our calculations indicate that the products lie 26.14 kcal/mol below the starting seven-membered rhodacycle **3-Cp**. Alternatively, the rhodium-hydride intermediate can reinsert into the olefin to lead to the formation of a six-membered rhodacycle **IntC-Cp** as shown in path ii. The reaction free energy and energy barrier were calculated to be –18.88 and 7.16 kcal/mol (**TS3**), respectively. Subsequently, **IntC-Cp** undergoes β -acetate elimination, resulting in the formation of **4a** and CpRh^{III}(OAc)₂ (**6-Cp**). The free energy of the resulting products is predicted to be 4.92 kcal/mol higher than that of **5aa** and **6'-Cp**. Notably, the Cp^X ligand exerts a significant impact on the thermodynamic stability of the final products (Fig. 3a). In particular, replacing the Cp ligand with Cp^{*} leads to a greater thermodynamic stability of the final products of path ii (–23.82 kcal/mol) than that of path i (–16.63 kcal/mol). This observation has been further confirmed by employing the Cp^{CF3} ligand. On the other hand, the optimized structures of **IntB-Cp^X** complexes with Cp, Cp^{CF3} and Cp^{*} ligands are presented in Fig. S15 (Supporting information). The Rh–H bond lengths follow the order of Cp^{*} (1.5544 Å) > Cp^{CF3} (1.5421 Å) > Cp (1.5387 Å), suggesting that the Rh–H bond in **IntB-Cp** are stronger than that in **IntB-Cp^{CF3}** and **IntB-Cp^{*}**. The HOMO and LUMO energy levels exhibit the trend of Cp=Cp^{CF3} > Cp^{*}, indicating that both Cp and Cp^{CF3} ligands are more electron-deficient than Cp^{*}, which further supports the relatively stronger Rh–H bonds in **IntB-Cp** and **IntB-Cp^{CF3}**. Overall, these findings could clearly explain the selective elimination of **3-Cp^X** as illustrated in Fig. 2.

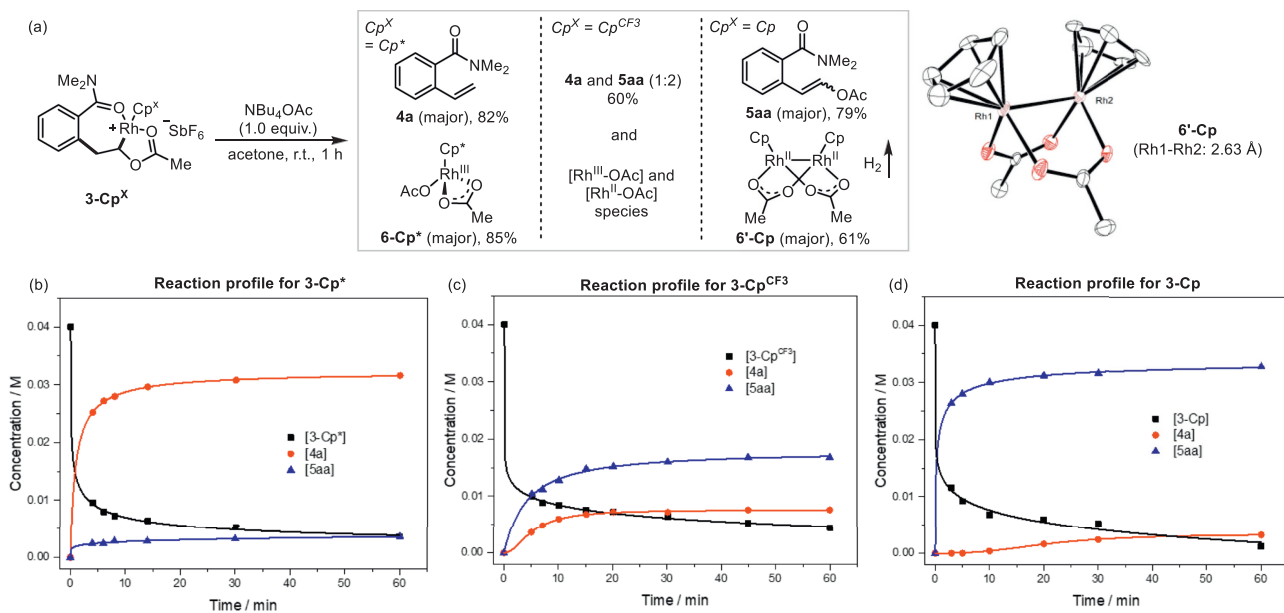


Fig. 2. (a) Selective eliminations of rhodacycles **3-Cp^X**. (b–d) Monitoring (¹H NMR) of the elimination of **3-Cp^X**.

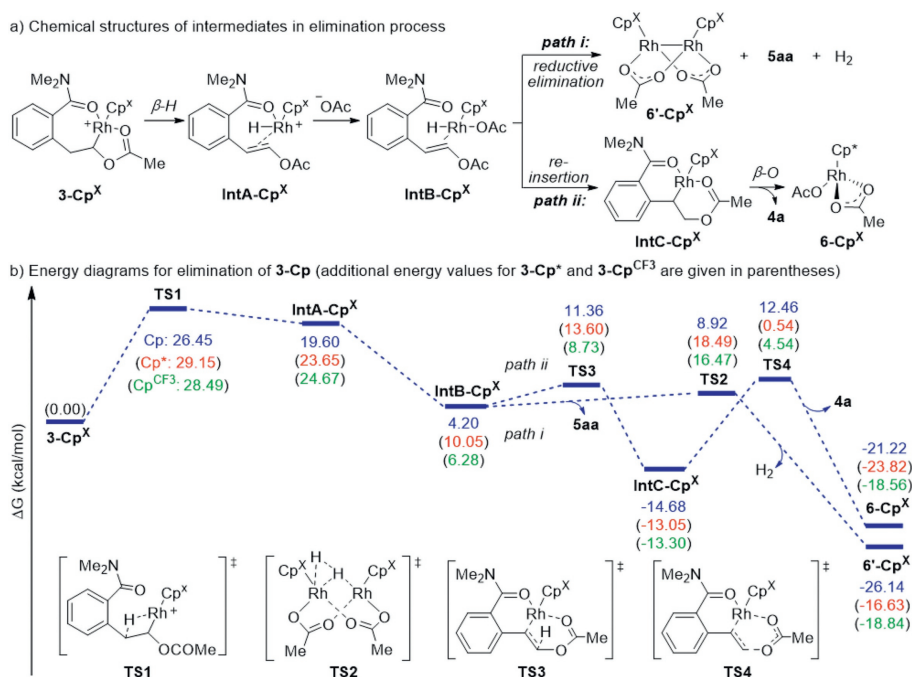


Fig. 3. Theoretical studies on elimination of **3-Cp^X**.

In order to investigate the effect of different Cp^X ligands on the C–H couplings of arenes with ethyl acrylate, catalytic reactions between benzamide **1b** and β,β -dideuterated ethyl acrylate **2b-d₂** were performed using three [Cp^XRh(MeCN)₃](SbF₆)₂ pre-catalysts (Cp^X=Cp*, Cp^{CF3} and Cp) (Fig. 4a). In the reaction catalyzed by electron-rich [Cp*Rh^{III}], considerable migrations of β -deuterium onto α -position of the olefination products **5bb-d** were observed, suggesting a β -H elimination/Rh–H olefin reinsertion sequence [45,46] in the catalytic cycle. On the contrary, no significant deuterium migrations were observed in reactions catalyzed by electron-deficient [Cp^{CF3}Rh^{III}] and [CpRh^{III}]. Similar observations were made in [Cp^XRh^{III}]-catalyzed C–H olefination of electron-rich acetanilide **1c** with β,β -dideuterated styrene **2c-d₂** (Fig. 4b). Un-

der catalytic reaction conditions, Rh-hydride olefin reinsertion was inhibited with electron-poor Cp^X ligands, possibly due to a facile β -H elimination/reductive elimination sequence.

To study the reaction mechanism, we thus conducted stoichiometric reactions of [Cp^{*}RhCl₂]₂, [Cp^{CF3}RhCl₂]₂, and [CpRhCl₂]₂ with benzamide **1a** and methyl acrylate **2d** in the presence of AgSbF₆ and NaOAc in acetone (Fig. 5a). Two six-membered rhodacycle complexes **7-Cp*** and **7-Cp^{CF3}** were isolated in good yields (73% and 70%). The ¹H NMR spectra of **7-Cp*** and **7-Cp^{CF3}** showed ddd multiplets (δ 4.25 (**7-Cp***) and 4.78 (**7-Cp^{CF3}**)) for methine groups connected to the rhodium centers. Along with these rhodacycles, the formation of the corresponding alkenylation product **5ad** (26% for [Cp*Rh]; 40% for [Cp^{CF3}Rh]) were observed. The

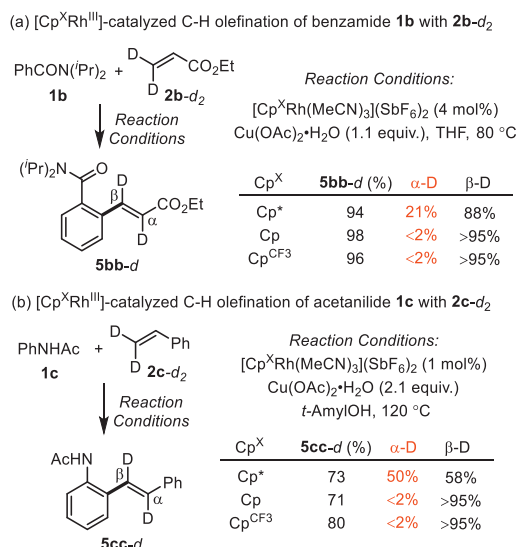


Fig. 4. Ligand-tuned product selectivity in Rh(III)-catalyzed C-H olefinations with ethyl acrylate and styrene.

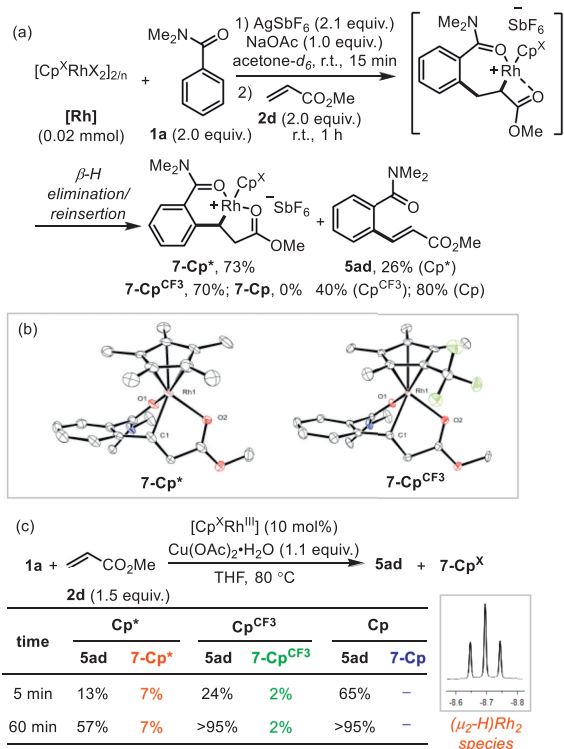


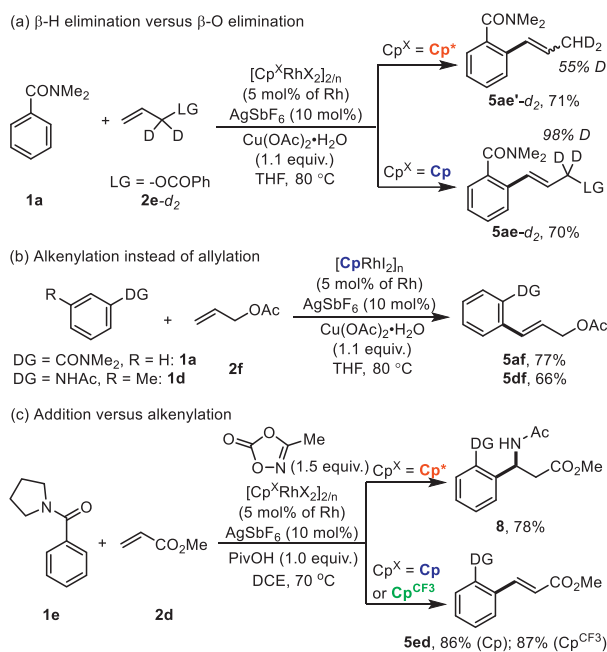
Fig. 5. (a) Syntheses of six-membered rhodacycles **7-Cp*** and **7-Cp^{CF3}**. (b) X-ray crystal structures of **7-Cp*** and **7-Cp^{CF3}**. Thermal ellipsoids are drawn at 50% probability. H atoms and SbF₆⁻ anions have been omitted for clarity. (c) Detection of catalytic species relevant to [Cp^XRh-H] intermediates.

alkenylation reactions of **1a** with **2d** in the presence of 4 mol% of **7-Cp*** and **7-Cp^{CF3}** were then conducted, both of which resulted in the desired **5ad** in good yields (Scheme S2 in Supporting information). However, the stoichiometric reaction of [CpRh]₂ with **1a** and **2d** directly afforded the alkenylation product **5ad** in 80% yield (Fig. S6 in Supporting information). In this case, we did not observe any specific rhodium complexes related to the expected six-membered rhodacycle complex **7-Cp**. The structures of **7-Cp*** and **7-Cp^{CF3}** were unambiguously confirmed by single-

crystal X-ray diffraction analyses (Fig. 5b), which showed selective [1,1]-insertion of methyl acrylate **2d** into the Rh-C bonds. Jones *et al.* previously established an analogous [1,1]-insertion process in reactions of cyclometalated rhodium complexes with ethylene and proposed a [1,2]-insertion/β-H elimination/Rh-H olefin reinsertion mechanism [45,46]. Here, the isolation of [1,1]-insertion products instead of the [1,2]-insertion counterparts could be attributed to the preference of six-membered-ring metallacycles over seven-membered-ring metallacycles. And the direct formation of **5ad** instead of **7-Cp** confirmed significant ligand effects on the reactivities of corresponding Rh-H intermediates.

The progress of the catalytic reactions of **1a** and **2d** with three [Cp^XRh^{III}] precatalysts (10 mol%) were further monitored utilizing ¹H NMR spectroscopy (Fig. 5c and Table S4 in Supporting information). The results showed that the [CpRh^{III}]-catalyzed alkenylation is much faster than [Cp^{*}Rh^{III}]- or [Cp^{CF3}Rh^{III}]-catalyzed reactions. And for the reaction catalyzed by [Cp^{*}Rh^{III}], **7-Cp*** was the major rhodium species (7%) observed after 5 min, along with a minor amount of (μ₂-H)Rh₂ species. As shown in Fig. 5c, the (μ₂-H)Rh₂ species displays an evident triplet resonance (*J* = 26 Hz) in the hydride region (δ = -8.7), confirming its presence [47,48]. On the other hand, for the reaction catalyzed by [Cp^{CF3}Rh^{III}], only 2% of **7-Cp^{CF3}** was formed after 5 min, accompanied by several other unknown rhodium species (Supporting information). Because **7-Cp^X** might be formed *via* the Rh-H olefin reinsertion step, they can be considered as alternate forms of corresponding rhodium hydride intermediates in the catalytic cycle. The concentrations of **7-Cp*** and **7-Cp^{CF3}** hardly varied with the reaction time. For the reaction catalyzed by [CpRh^{III}], we did not detect any signals belonging to **7-Cp** or Rh-H species. These results confirmed more facile reductive elimination of the Rh-H intermediates with electron-deficient Cp^X ligands.

In Heck-type reactions, reinsertion of alkenes into metal hydride intermediates may result in undesired olefin isomerizations. However, in transformations like Sigman's asymmetric redox-relay oxidative Heck reactions [18,19], iterative β-hydride elimination/migratory insertion processes are promoted to achieve high selectivities. The knowledge of electronic ligand effects on β-H elimination/reductive elimination sequence can be utilized to customize catalytic systems for different needs. To this end, several arene-alkene coupling reactions were tested using different [Cp^XRh] catalysts (Scheme 2). Allylic surrogates, as unsaturated coupling partners, typically undergo direct C(sp²)-H allylation (*via* β-O or β-X elimination) instead of Heck-type olefination reaction (*via* β-H elimination) [49]. The catalytic reactions of benzamide **1a** with allylic electrophile **2e-d₂** were conducted (Scheme 2a). [Cp^{*}Rh^{III}] led to **5ae'-d₂** in 71% yield with excellent β-OCOPh elimination, while electron deficient [CpRh^{III}] selectively led to **5ae-d₂** by β-H elimination. The deuterium-labelling results indicate that the reactions proceeded with complete γ-selectivity, ruling out the possibility of an oxidative addition of the allyl electrophile to Rh^{III} centers. The [Cp^{*}Rh]-catalyzed direct C(sp²)-H bond allylation with allyl acetate have already been widely explored [50,51]. However, in the presence of [CpRh^{III}] catalyst, dehydrogenative C-H alkenylation reactions of benzamide **1a** and acetanilide **1d** with allyl acetate **2f** proceeded smoothly (Scheme 2b), affording **5af** and **5df** in good yields (77% and 66%, respectively). [Cp^XRh^{III}]-catalyzed coupling reactions between benzamide **1b** and methyl acrylate **2d** were also tested using 3-methyl-1,4,2-dioxazol-5-one [17] as an oxidant (Scheme 2c). Under [Cp^{*}Rh^{III}] catalysis, the reaction afforded α-branched amine product **8** in 78% yield *via* an oxidative interception [52,53] of a [1,1]-insertion intermediate analogous to **7-Cp***. In contrast, under [Cp^{CF3}Rh^{III}] or [CpRh^{III}] catalysis, alkenylation product **5ed** was yielded selectively, indicating much more facile β-H elimination/reductive elimination of corresponding alkene insertion intermediates. The catalytic performance of



Scheme 2. Examples for Cp^X ligand-tuned divergent arene-alkene coupling reactions.

$[\text{Cp}^*\text{Rh}^{\text{III}}]$, $[\text{Cp}^{\text{CF}_3}\text{Rh}^{\text{III}}]$ and $[\text{CpRh}^{\text{III}}]$ in these reactions is consistent with the insights gained from the mechanistic studies.

In summary, we have investigated the impact of three representative Cp^X (Cp^* , Cp^{CF_3} and Cp) ligands on rhodium(III)-catalyzed arene-alkene coupling reactions. The successful isolation and characterization of seven-membered rhodacycles **3-Cp***, **3-Cp^{CF}** and **3-Cp**, as well as six-membered rhodacycles **7-Cp*** and **7-Cp^{CF}**, confirm the relationship between [1,2]-insertion and [1,1]-insertion processes. The experimental and theoretical studies on chemoselective eliminations of different **3-Cp^X**, along with the isolation of corresponding Rh(III) complex **6-Cp*** and dimeric Rh(II) complex **6'-Cp**, demonstrates the significant impact of electronic ligand effects on product selectivity. These findings, together with the ligand-directed divergent coupling reactions of arenes with diverse alkenes, support the conclusions that (i) Rh(III) centers with electron-deficient ligands can facilitate β -H elimination/reductive elimination sequences, (ii) Rh(III) centers with electron-rich ligands can enable rhodium-migration. These mechanistic insights into ligand effects provide a roadmap for the rational design of increasingly efficient catalyst systems for C-C bond formation reactions.

Declaration of competing interest

The authors declare that they have no known competing financial interests or personal relationships that could have appeared to influence the work reported in this paper.

Acknowledgments

We thank the financial support from the National Natural Science Foundation of China (Nos. 21772162, 21772165, 22171237, 22071208) and Youth Innovation foundation of Xiamen (No. 3502Z20206058).

Supplementary materials

Supplementary material associated with this article can be found, in the online version, at doi:10.1016/j.ccl.2023.108906.

References

- [1] J.L. Bras, J. Muzart, *Chem. Rev.* 111 (2011) 1170–1214.
- [2] C. Liu, J.W. Yuan, M. Gao, et al., *Chem. Rev.* 115 (2015) 12138–12204.
- [3] G.Y. Song, X.W. Li, *Acc. Chem. Res.* 48 (2015) 1007–1020.
- [4] C.S. Yeung, V.M. Dong, *Chem. Rev.* 111 (2011) 1215–1292.
- [5] R. Logeswaran, M. Jeganmohan, *Adv. Synth. Catal.* 364 (2022) 2113–2139.
- [6] R.D. Baxter, D. Sale, K.M. Engle, J.Q. Yu, D.G. Blackmond, *J. Am. Chem. Soc.* 134 (2012) 4600–4606.
- [7] M. Brasse, J. Campora, J.A. Ellman, R.G. Bergman, *J. Am. Chem. Soc.* 135 (2013) 6427–6430.
- [8] A. Deb, A. Hazra, Q. Peng, R.S. Paton, D. Maiti, *J. Am. Chem. Soc.* 139 (2017) 763–775.
- [9] J. Kim, S.W. Park, M.H. Baik, S. Chang, *J. Am. Chem. Soc.* 137 (2015) 13448–13451.
- [10] P. Wang, P.V. Erma, G.Q. Xia, et al., *Nature* 551 (2017) 489–493.
- [11] S.L. Zhang, L. Shi, Y.Q. Ding, *J. Am. Chem. Soc.* 133 (2011) 20218–20229.
- [12] Y.T. Li, H. Shi, *Chin. Chem. Lett.* 35 (2024) 108650.
- [13] D. Fiorito, S. Scaringi, C. Mazet, *Chem. Soc. Rev.* 50 (2021) 1391–1406.
- [14] H.E. Bonfield, D. Valette, D.M. Lindsay, M. Reid, *Chem. Eur. J.* 27 (2021) 158–174.
- [15] Y. Li, D. Wu, H.G. Cheng, G. Yin, *Angew. Chem. Int. Ed.* 59 (2020) 7990–8003.
- [16] A. Vasseur, J. Bruffaerts, I. Marek, *Nat. Chem.* 11 (2016) 209–219.
- [17] S. Maity, T.J. Potter, J.A. Ellman, *Nat. Catal.* 2 (2019) 756–762.
- [18] W. Werner, T.S. Mei, A.J. Burckle, M.S. Sigman, *Science* 338 (2012) 1455–1458.
- [19] J.B. Liu, Q.J. Yuan, F.D. Toste, M.S. Sigman, *Nat. Chem.* 11 (2019) 710–715.
- [20] C. Romano, D. Fiorito, C. Mazet, *J. Am. Chem. Soc.* 141 (2019) 16983–16990.
- [21] N. Wagner-Carlberg, T. Rovis, *J. Am. Chem. Soc.* 144 (2022) 22426–22432.
- [22] D. Wu, H.L. Pang, G.Y. Yin, *Chin. Chem. Lett.* 34 (2023) 108087.
- [23] S. Kim, F. Loose, M.J. Bezdek, X.P. Wang, P.J. Chirik, *J. Am. Chem. Soc.* 141 (2019) 17900–17908.
- [24] Y.J. Wang, L. Zhu, Z.H. Shao, et al., *J. Am. Chem. Soc.* 141 (2019) 17337–17349.
- [25] K. Tanaka, *Rhodium Catalysis in Organic Synthesis: Methods and Reactions*, Wiley-VCH, 2019.
- [26] T. Piou, T. Rovis, *Acc. Chem. Res.* 51 (2018) 170–180.
- [27] F.W. Patureau, T. Besset, F. Glorius, *Angew. Chem. Int. Ed.* 50 (2011) 1064–1067.
- [28] Y. Takahama, Y. Shibata, K. Tanaka, *Chem. Eur. J.* 21 (2015) 9053–9056.
- [29] K.D. Otley, J.A. Ellman, *Org. Lett.* 17 (2015) 1332–1335.
- [30] W. Lin, W. Li, D. Lu, et al., *ACS Catal.* 8 (2018) 8070–8076.
- [31] J. Tanaka, Y. Nagashima, K. Tanaka, *Org. Lett.* 22 (2020) 7181–7186.
- [32] Y. Nagashima, S. Ishigaki, J. Tanaka, K. Tanaka, *ACS Catal.* 11 (2021) 13591–13602.
- [33] Q. Zhang, H.Z. Yu, Y.T. Li, et al., *Dalton Trans.* 42 (2013) 4175–4184.
- [34] P.G. Gassman, J.W. Mickelson, J.R. Sowa Jr., *J. Am. Chem. Soc.* 114 (1992) 6942–6944.
- [35] T. Piou, F. Romanov-Michailidis, M. Romanova-Michaelides, et al., *J. Am. Chem. Soc.* 139 (2017) 1296–1310.
- [36] N. Dunwoody, S.S. Sun, A.J. Lees, *Inorg. Chem.* 39 (2000) 4442–4451.
- [37] L. Li, W.W. Brennessel, W.D. Jones, *J. Am. Chem. Soc.* 130 (2008) 12414–12419.
- [38] L. Li, W.W. Brennessel, W.D. Jones, *Organometallics* 28 (2009) 3492–3500.
- [39] Y. Li, X.S. Zhang, H. Li, et al., *Chem. Sci.* 3 (2012) 1634–1639.
- [40] M.E. Tauchert, C.D. Incarvito, A.L. Rheingold, R.G. Bergman, J.A. Ellman, *J. Am. Chem. Soc.* 134 (2012) 1482–1485.
- [41] Y. Hu, J.R. Norton, *J. Am. Chem. Soc.* 136 (2014) 5938–5948.
- [42] B.R. James, D. Mahajan, S.J. Rettig, G.M. Williams, *Organometallics* 2 (1983) 1452–1458.
- [43] C. Bruneau, P.H. Dixneuf, *Ruthenium(II)-Catalyzed Functionalisation of C-H Bonds With Alkenes: Alkenylation versus Alkylation*, Topics in Organometallic Chemistry, Springer, 2015.
- [44] Gaussian 16, Revision A.03, Gaussian, Inc., Wallingford CT, 2016.
- [45] L. Li, Y. Jiao, W.W. Brennessel, W.D. Jones, *Organometallics* 29 (2010) 4593–4605.
- [46] Y.F. Han, G.X. Jin, *Chem. Soc. Rev.* 43 (2014) 2799–2823.
- [47] C. White, A.J. Oliver, P.M. Maitlis, *Dalton Trans.* (1973) 1901–1907.
- [48] F.L. Taw, H. Mellows, P.S. White, et al., *J. Am. Chem. Soc.* 124 (2002) 5100–5108.
- [49] S. Dutta, T. Bhattacharya, D.B. Werz, D. Maiti, *Chem* 7 (2021) 555–605.
- [50] N.K. Mishra, S. Sharma, J. Park, S. Han, I.S. Kim, *ACS Catal.* 7 (2017) 2821–2847.
- [51] H. Wang, N. Schröder, F. Glorius, *Angew. Chem. Int. Ed.* 52 (2013) 5386–5389.
- [52] A.D.S. Dipannita Kalyani, M.S. Sanford, *J. Am. Chem. Soc.* 132 (2010) 8419–8427.
- [53] T. Pinkert, T. Wegner, S. Mondal, F. Glorius, *Angew. Chem. Int. Ed.* 58 (2019) 15041–15045.